NASA Contractor Report CR 189054

Evaluation of In-Situ Thermal Energy Storage for Lunar Based Solar Dynamic Systems

Roger A. Crane
The University of South Florida
Tampa, Florida

March 1991

Prepared for
Lewis Research Center
Under Grant NAG3-851

NASA

National Aeronautics and
Space Administration

Table of Contents

Table of Figures

Tables

1. INTRODUCTION

This report will describe the work on an ongoing effort conducted at the University of South Florida in regard to the development of Thermal Energy Storage (TES) concepts as applied to advanced solar dynamic power systems. The range of interest within NASA for such designs has included both orbiting space systems and a lunar based system. Work in both areas has been undertaken. Through this report, results of a feasibility evaluation of a lunar based thermal energy storage system is presented.

A practical lunar based thermal energy storage system, based on locally available materials, could significantly reduce transportation requirements and associated costs of a continuous, solar derived power system. One proposal for such a concept was developed at the University of South Florida in collaboration with engineers and scientists at the NASA Lewis Research Center. This concept is based on a unique, in-situ approach to thermal energy storage. In this study the proposed design is examined to access the problems of start-up and the requirements for attainment of stable operation. The design remains, at this stage, partially conceptional in nature, but certain aspects of the design, bearing directly on feasibility, are examined in some detail. Specifically included is an engineering evaluation of the projected thermal performance of this system. Both steady state and start-up power requirements are evaluated and the associated thermal losses are evaluated as a basis for establishing potential system performance.

2. LUNAR BASED SOLAR DYNAMIC POWER GENERATION

During an earlier study [1], a lunar based focused concentrator was evaluated for providing high temperature process heat. The system was to operate in conjunction with a Solar Dynamic Power Generation (SDPG) unit to provide additional electrical power. This co-generation concept was presented as a limited alternative to an all electric power system based on the already well developed, space proven, photovoltaic (PV) power array. An advanced fuel cell would be incorporated with the PV array for the extended periods where direct solar energy was unavailable.

Much of the incentive for the solar dynamic alternative was thought to be related to the substantial efficiency gain when process heating is obtained directly, without the intermediate conversion to electrical power. The approach taken was to adapt the SDPG technology developed earlier for Low Earth Orbit (LEO) to make it suitable for the lunar environment. During this study it became apparent that, because of the relatively long periods of solar eclipse, the problem of providing continuous electrical power generation on the lunar surface is fundamentally different that those problems encountered in LEO so that a fresh look at overall optimal system design under the lunar imposed constraints is needed. In LEO the typical solar eclipse period is of the order of 36 minutes. In order to provide a continuous source of energy to the system, the LEO receiver was be designed to include Thermal Energy Storage (TES) material. Because of the substantial mass of material required for thermal storage, the LEO receiver will typically become the single heaviest system component, providing on the order of 45% [2] of overall system weight. The lunar day/night period includes a 354 hour eclipse. Periods without direct solar incidence on the moon are greater by nearly a factor of 600. Energy storage, previously significant in the design of LEO systems, then becomes the dominant factor in any lunar solar based power system, largely determining both weight and costs. The advantage that SDPG offers is the potential for replacing the rather complex earth produced fuel cell storage system with a thermal storage system utilizing native, processed or unprocessed materials. Reductions in the required transport charges for the co-generation system were found to be as large as 67%, indicating that such a system could offer substantial costs advantages over the best alternative solar technologies. On this basis it was decided to explore the alternative of SDPG as an electrical production source independent from any process heat application.

As will be noted, any of the economically competitive solar technologies will involve the development of new technologies and, as a consequence, incorporate a

degree of development risk. The long term operation of a high temperature fuel cell with oxygen and hydrogen cryogenic storage under low maintenance conditions has not been demonstrated to date; similarly, SDPG, while having undergone substantial development work, remains a largely unproven technology. Most notable in this regard will be those technologies which rely on the properties of the lunar storage material itself. In particular, there are basic concerns about the high temperature requirements imposed by the concept. The system must operate near the limits of currently demonstrated metallurgical capability. Long term, low maintenance operation of such a system has not been demonstrated.

This study was established for the purpose of evaluating a SDPG system designed exclusively for the purpose of electrical power generation. A proposed configuration will be presented and technological barriers identified. The intention is to provide a basis for risk assessment and benefit analysis. It is also intended to identify technological development requirements needed to permit near term development and testing of such a system.

2.1 SOLAR DYNAMIC SYSTEM REQUIREMENTS

Solar Dynamic Power Generation systems have been extensively studied [3, 4] for applications in LEO, being generally sized to provide between 1.5 and 35 kW_e. The upper size limitation is attributed to the difficulty of fabricating very large concentrators with the requisite surface accuracy. Greater power requirements can be supplied by assembling several modules into a single unit. The design being developed here may require somewhat higher concentration ratios than these earlier LEO designs due to the high melting temperatures of the lunar soil. Further, the increased period during which the system is eclipsed will place greater demands on the solar concentrator. This suggests that these units should be sized somewhat below the larger 35 kW_e units; these considerations, together with the large number of studies in the Advanced Solar Dynamic Power Generation program concentrating on the 25 kW_e units, have led to a selection of the 25 kW_e unit as the standard for this study.

NASA has previously considered three basic power cycles [2] in conjunction with solar dynamic systems: (a) Brayton cycles, (b) Stirling cycles and (c) Rankine cycles. After the initial development effort the Rankine cycle was dropped from consideration and a major emphasis was placed on the development of a suitable Stirling cycle. While the Stirling cycle remains, perhaps, the major contender, the Brayton cycle is thought to

provide a more conservative standard of comparison. Estimations of Stirling cycle efficiency, while higher, have frequently been difficult to predict with sufficient confidence. By introducing the Brayton cycle as a standard of evaluation in this study the associated uncertainties of the Stirling engine are avoided so that more definitive conclusions might be reached; results may be somewhat improved in the event that a Stirling cycle is substituted.

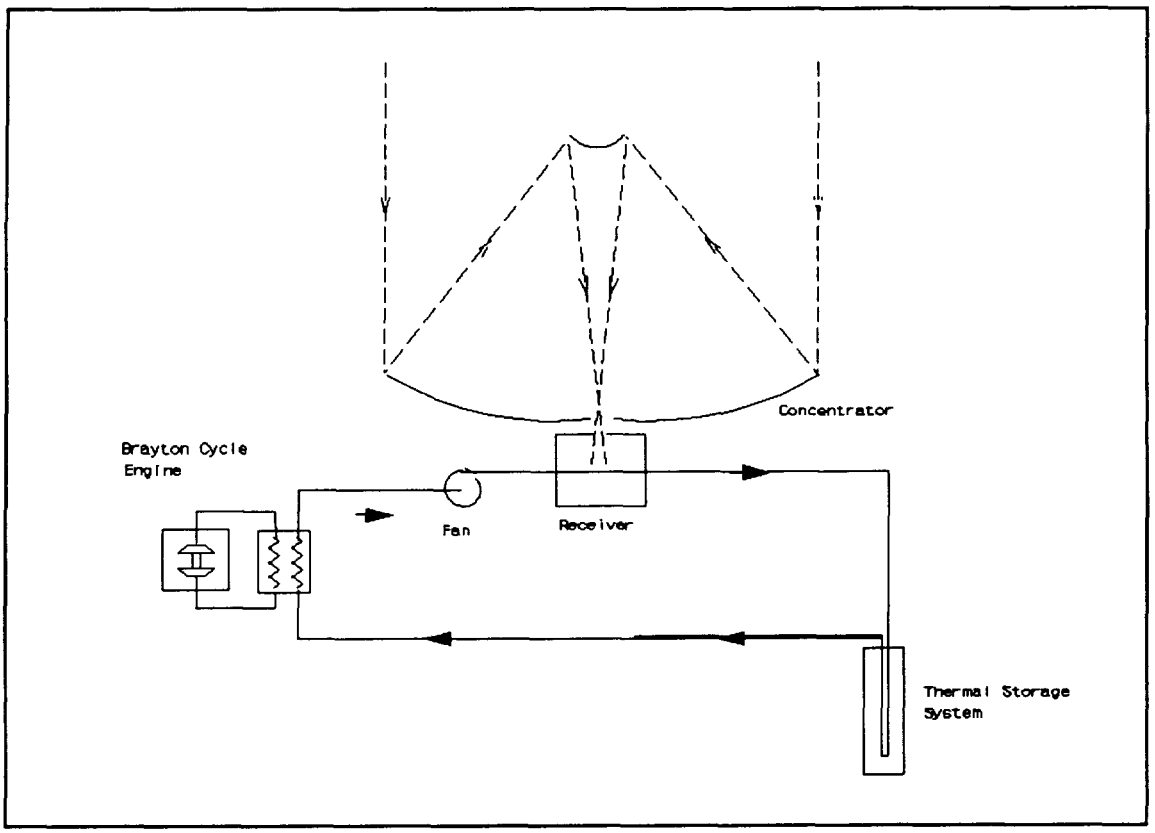

Figure 1. Solar Dynamic Power System.

The proposed electrical generation system arrangement is shown schematically in Figure 1. The arrangement shown is typical of SDPG systems; the unique feature of this concept is the use of a native lunar thermal storage material (TSM) which may be utilized in-situ. The system utilizes a circulating helium-xenon mixture to transport heat between the concentrator, TSM and Brayton engine. Helium-xenon mixtures have frequently been proposed for SDPG in that they result in a mixture with relatively high specific kinetic energy and high convective coefficients. Since the circulating gas does not pass through the turbine only the high convective coefficients and the chemical inertness are required here suggesting that pure helium might provide better heat transport properties. However the density of helium is quite low at moderate pressures.

Preliminary calculations have indicated that this leads to either a higher pressure system or larger piping to maintain reasonable mass flows. The decision has been made to work with a helium-xenon mixture similar to that proposed for the working fluid in the Brayton cycle. The mixture will have an equivalent molecular weight of 38, so that properties for this mixture are used in all calculations.

The decision to use native materials limits the choice of a TSM. Moreover it tends to limit the choice in system operating temperatures to match those characteristics of the available rock. While the lunar surface contains a variety of mineral and mineral ores, much of the surface is of volcanic origin. The mare regions, which are sufficiently large to be one of the first identifiable features of the lunar surface, are considered to have been formed from volcanic outflows. Basaltic rocks provide a common material with relatively well understood physical properties. Properties are not necessarily similar to those of related earth rocks, but previous Apollo missions have provided sufficient samples to provide a partial estimation of transport properties. Basaltic ores are found in a large number of lunar sites so that their selection as a TSM provides a high degree of flexibility in the siteing of such a system. As with most raw materials, these ores are composed of a variety of chemical compounds. Such materials will be characterized as having physical properties which vary with the site. Also characteristic of such materials is that the melting properties are not sharp, that is, they will gradually melt over a temperature range rather than at a specific single temperature.

A TSM may utilize either sensible or latent energy, or perhaps a combination of the two, but it is generally recognized as advantageous to utilize the phase transition. In doing so the range of temperature swings, which the thermodynamic cycle must undergo, is limited. Basaltic rocks will, due to their variable composition, melt over a range of temperatures forming a variety of crystals. Major classifications of crystals include olivine, plagioclase, pyroxene and ilmenite. Crystallization curves from the Apollo 12 Basalts are shown in Figure 2. Note that these samples differ noticeably within the melting range. Each begins to melt at temperatures between 1325 and 1350 K, but complete melting temperatures range from between 1425 and 1675 K. The curve for sample 12021, notable for the low Mg to Mg+Fe ratio, indicated the narrowest temperature swing and the lowest total melting temperature. Taylor [5] suggests that each of these curves for differing samples might be reduced to a single curve by the removal or addition of MgO. In so doing the relative portions of normative olivine, pyroxene, plagioclase and ilmenite change. Olivine basalt, characterized in soil samples by the presence of larger portions of MgO, is seen to be associated with the higher

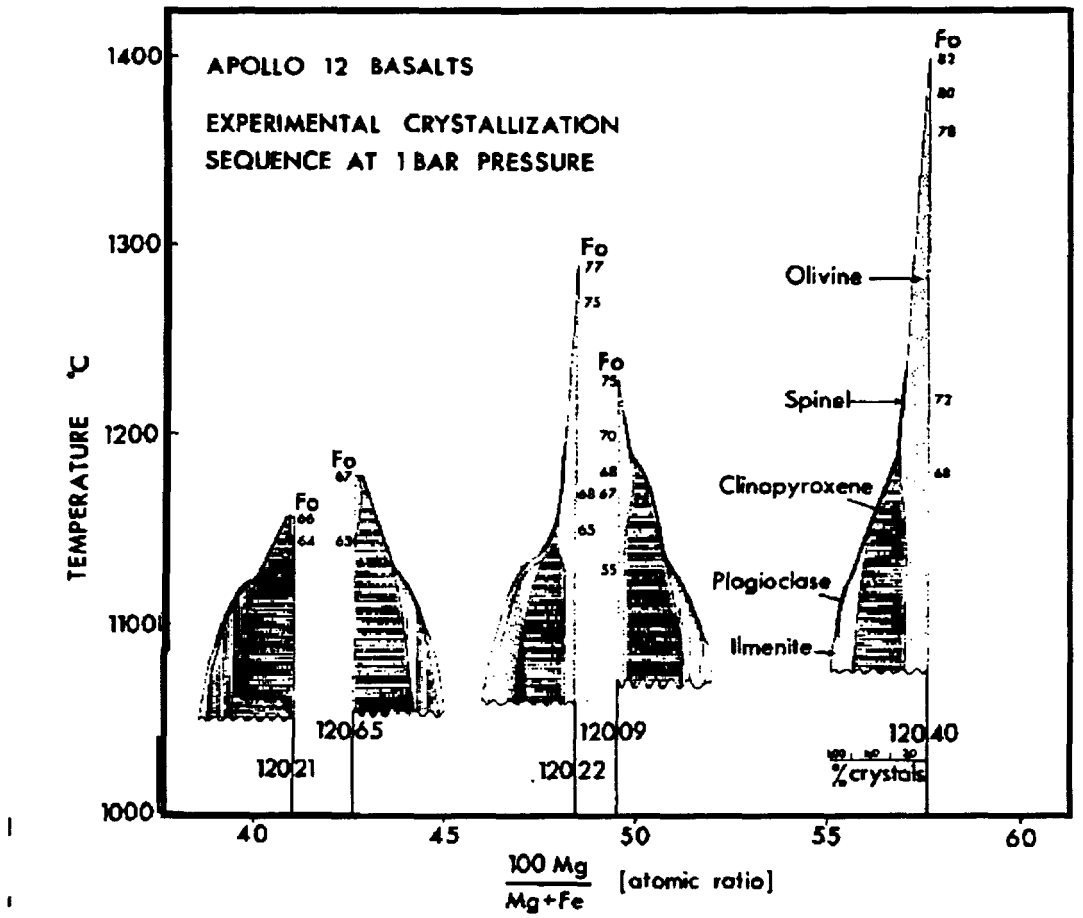

Figure 2. Crystallization Curves for Apollo 12 Rock Samples. [5]

melting temperature. Minear et. al. [6] noted that the latent heat of crystallization will also differ with the crystalline formation. This variation is shown in Table I.

The overall thermal transport properties of the regolith will obviously depend on the mineralogy of the specific site. Herbert et. al. [7] note that high olivine basalts have an unusually high heat of fusion, around 862 kJ/kg. It would seem that if sites could be found with a near optimal composition, thermal storage could be made relatively efficient. If consideration is limited to those soils determined to have a very low MgO content, then TSM temperatures may be restricted to a range between 1325 and 1425 K. This selection provides not only the lowest temperature swing but also the lowest peak temperature. Since both characteristics are judged desirable, sites considered in this analysis will be limited to these areas.

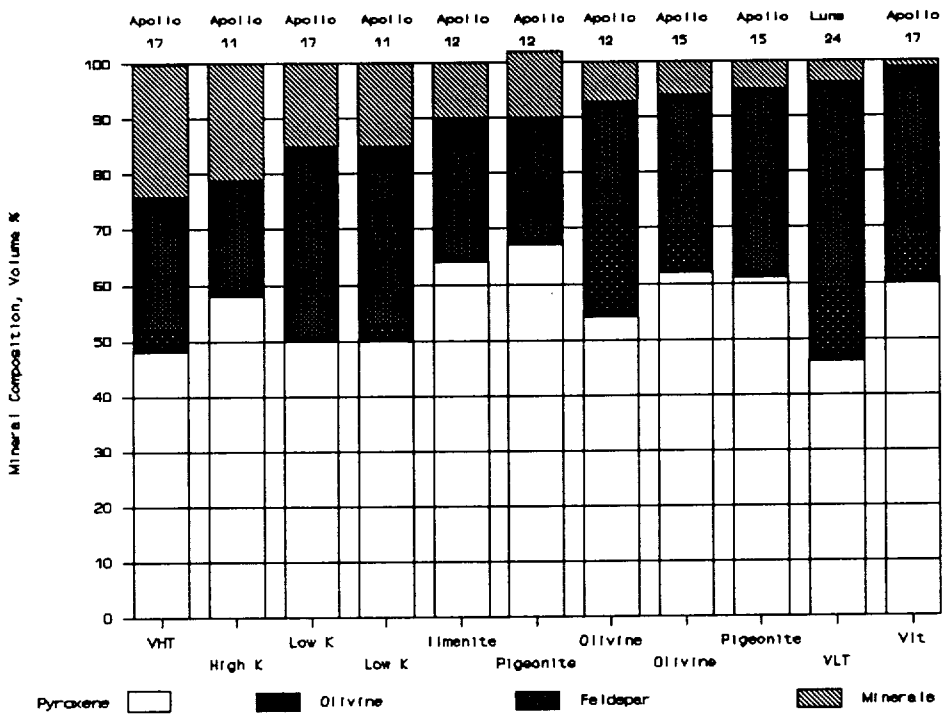

Figure 3. Modal Mineral Content in a Range of Lunar Mare Basalts. [8]

TABLE I. Latent Heat of Crystallization for Basaltic Rocks

	Latent Heat J/kg/K	Conductivity W/m/K	Density kg/m^3
Olivine Basalts			3400
Forsterite	950	5.0	3035
Fayalite	453	3.2	3764
Pyroxene Basalts			
Enstatite	699	4.4	
Wollanstonite	590	4.0	2846
Ferrosilite	699		
Plagioclase Basalts			2700
Albite	208	2.3	
Anorthite	270	1.7	
Ilmenite	650	2.6	

The question of whether low MgO sites might be found in the vicinity of ilmenite mining regions should be considered. Heiken et. al. [8] noted that "Ilmenite ... consists of alternating layers of Ti- and Fe-containing octahedra. Most lunar ilmenite contains some Mg substituting for Fe which arises from the solid solution that exists between ilmenite (FeTiO3) and MgTiO3...", suggesting that the two compounds are generally found together. However, as seen in Figure 3, samples at both the Apollo 11 and 17 sites, where the major mining effort might be expected, show locations without appreciable olivine basalt presence. The presence of such sites in the limited number of sampling taken would indicate that they are probably not rare. In the event that later evaluation of data indicate the desirability of operation in regions of high MgO content, it is noted that the unusually high heat of fusion of these soils would tend to offset the higher melting range so that qualitatively similar system performance might be anticipated.

The temperatures being proposed are substantially higher than were considered for SDPG units operating in LEO. As a result, they will present a new set of technological problems if latent storage is selected. However the proposed temperature level of 1425 K is still below the design limit of certain high temperature alloys currently used or being tested for aircraft engines. Moreover the lunar soils are highly reduced so that much of the high temperature corrosion problem may not be severe. Certainly additional experimental evaluation of this aspect of the design would be in order. The demonstration of the performance of these alloys or the selection of new, more suitable, materials will be one of the more significant technological development requirements for the overall system. In the case that problems are encountered in developing suitable high temperature alloys, sensible energy storage at lower temperature levels remains an alternative. Should a sensible energy storage design be selected, the system will continue to operate in substantially the same manner, but at a penalty to the overall system efficiency.

2.2 BRAYTON CYCLE PERFORMANCE

In order to establish the TES requirements, the overall thermodynamic efficiency of the Brayton cycle engine must be known. Performance has been determined using typical component efficiencies and applying basic thermodynamic relationships. In this case the efficiencies have been extracted from the Advanced SDPG Base Line design [3] as shown in Table II. Portions of this data have been extrapolated. Certain

alterations have been made; most notable have been the downward adjustment of the recuperator efficiency from 0.95 to 0.90 and with the Compressor ratio being increased accordingly. Neither change may be regarded directly as an optimization; rather they are an attempt to indicate performance near what may be regarded as nominal design conditions.

In this design it is assumed that no compressor gas is diverted for turbine cooling. The inert gas mixture used as a working fluid is thought to permit the use of refractory metals for high temperature engine components. The 2% compressor bleed stream is used for the gas bearings.

The procedure for extrapolating performance has been to hold each of the thermodynamic parameters constant in the cycle analysis, except for the TSM temperature and radiator efficiency. The peak cycle temperature is calculated based on the receiver efficiency. Gas leaving the receiver has a temperature increase equivalent to 86% of the temperature difference between receiver gas inlet temperature and the TSM temperature. Similarly, gas entering the radiator is cooled to 59% (56% for sensible storage) of the temperature difference between the inlet gas temperature and that of space. In evaluating the effects of changing TSM temperature, the radiator efficiency has been adjusted simultaneously to ensure a closed cycle.

TABLE II. BRAYTON CYCLE THERMODYNAMIC PARAMETERS

	Latent Storage	Sensible Storage
Specific Heat Ratio	1.665	1.665
Compressor Pressure Ratio	2.00	1.80
Turbine Pressure Ratio	0.61	0.61
Compressor Efficiency	0.80	0.80
TES Heat Exchanger Efficiency	0.86	0.86
Turbine Efficiency	0.76	0.76
Radiator Efficiency	0.59	0.56
Temp. of Space	191 K	191 K
Compressor Bleed	0.20 %	0.20 %
Recuperator Efficiency	0.90 %	0.90 %
Mechanical Efficiency	0.99 %	0.99 %
Alternator Efficiency	0.92 %	0.92 %

The cycle temperature and pressure conditions corresponding to a 1325 K and a

1250 K TSM temperature and a 93% recuperator efficiency are shown in Table III. The higher temperature corresponds to a temperature attainable with melting of the TSM. The 1250 K case corresponds to a case in which melting is not attained. The values are sufficiently close that only minor differences are seen in the overall Brayton cycle efficiencies. The overall efficiency of the latent storage system is calculated to be 31%, for the sensible storage system 30%. The effects of TSM temperature and recuperator efficiency on the Brayton Cycle efficiency are shown in Figure 4. Clearly there is a significant advantage to operating the cycle at as high a TSM temperature as possible. Similarly the efficiency of the recuperator is seen to be an important consideration in system efficiency and this importance continues over the entire temperature range of interest.

TABLE III. BRAYTON CYCLE THERMODYNAMIC CHARACTERISTICS

	Temperature, K		Pressure, atm.	
	in	out	in	out
TSM at 1325 K				
Compressor	331	463	15.48	30.96
Recuperator/Cold Side	463	985	27.69	27.42
Receiver	985	1277		
Turbine	1277	1043	26.23	16.00
Recuperator/Hot Side	1043	531	16.00	15.72
Radiator	531	331	15.72	15.55
Cycle Efficiency				0.34
Overall Efficiency				0.31
TSM at 1250 K				
Compressor	331	463	15.48	30.96
Recuperator/Cold Side	463	949	27.69	27.42
Receiver	949	1208		
Turbine	1208	986	26.23	16.00
Recuperator/Hot Side	986	510	16.00	15.72
Radiator	510	331	15.72	15.55
Cycle Efficiency				0.33
Overall Efficiency				0.30

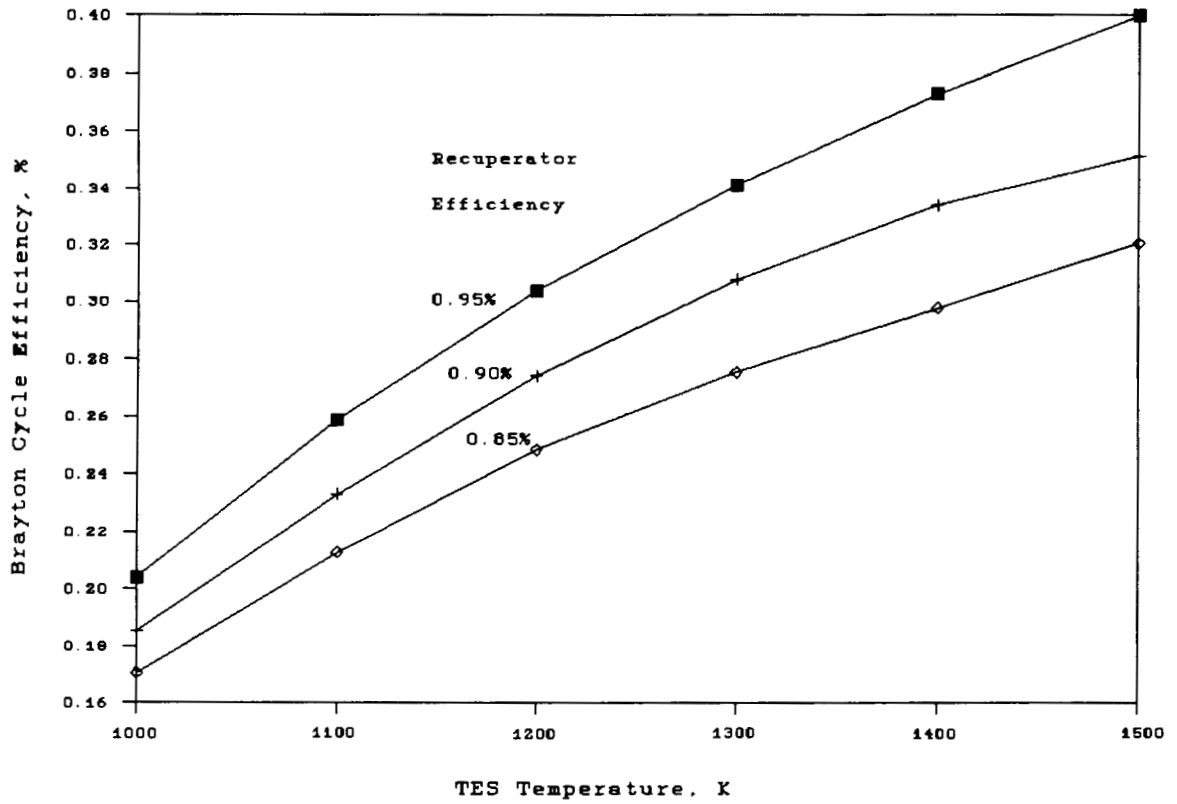

FIGURE 4. TES Temperature Effects on Brayton Cycle Efficiency.

2.3 THERMAL ENERGY STORAGE

Results of the process co-generation study indicated that the required volume of TSM would be sufficiently large to preclude other than local manufacture. The arrangement considered here utilizes a lunar TSM with its containment formed in place. One potential configuration is shown in Figure 5. The gaseous heat transport fluid flows through each of several helical annuli connected together through a manifold at the lunar surface. Holes are initially augured in the regolith to accommodate the coolant tubes of the TES. Such holes might alternately be formed by using a heated tip [9] boring device. Thermal losses through the fine powder under vacuum conditions should be relatively minor so that such procedures would be highly efficient.

After forming the hole to a suitable depth a two wall, capped helical spiralled tube is inserted. One side of the tube will serve to bring high temperature gas from the solar receiver, the second acts as a return. During the period of solar incidence, the high

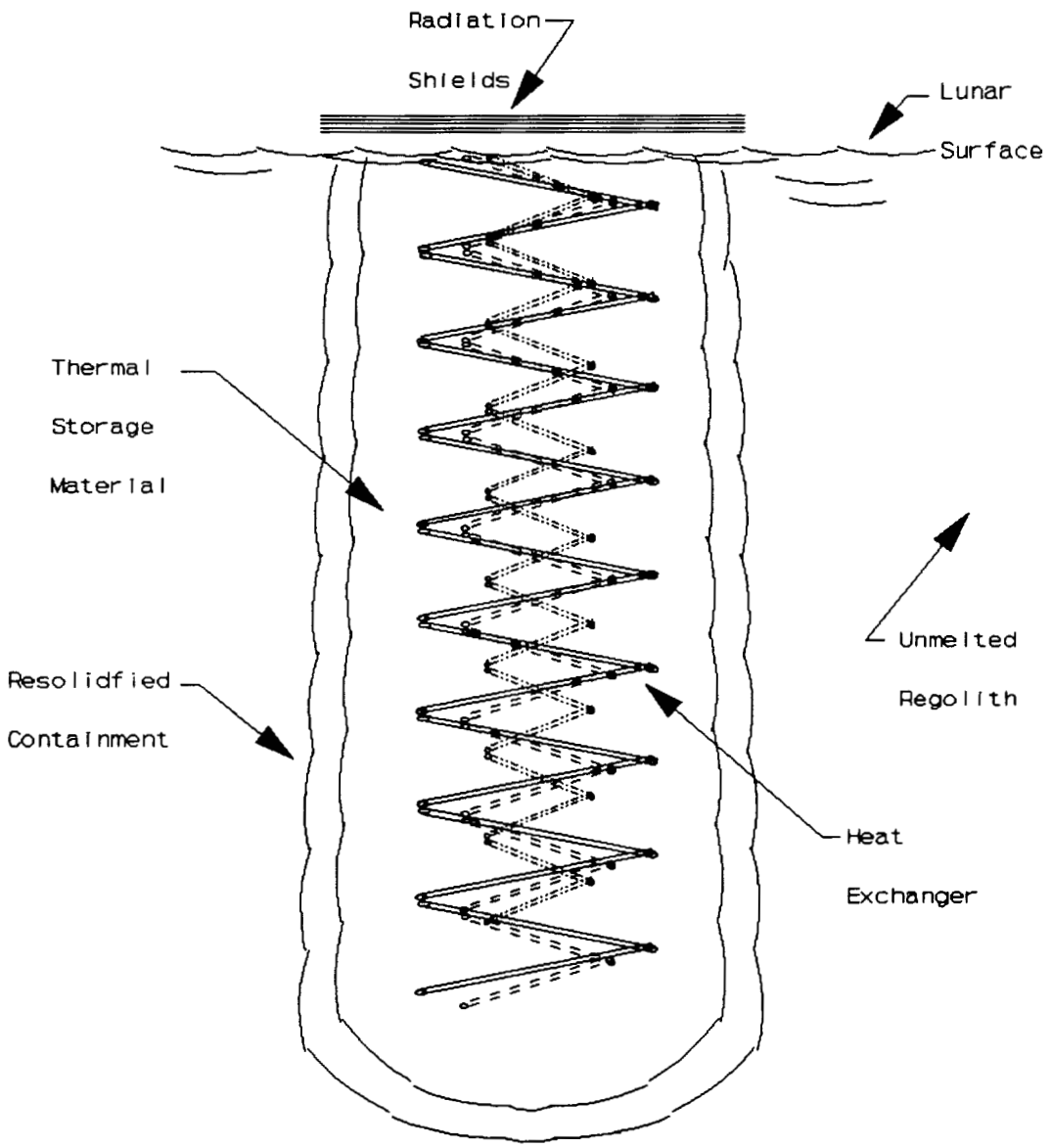

FIGURE 5. Proposed in-situ TES arrangement.

temperature gas will heat the adjacent rock and, if required, gradually cause melting. The melt front will continually expand increasing the volume of TSM. While molten material is somewhat viscous, particularly near the edge of the melt front, a portion of the material will gradually seep out of the melted zone and flow into the surrounding rock. There, molten material will be cooled and begin to re-solidify. With this process

a containment is formed in place. Densification will occur with the re-solidification of molten rock and the elimination of much of the original void space. The result is that latent storage results in a more compact storage arrangement but is likely to lead to a local subsidence effect and will require additions of material, perhaps from process spoils. This would help to ensure low oxygen fugacity, but care must be exercised to ensure against the introduction of higher olivine basalt content.

In order to keep the tube centered in the melted pool an extended tip may be added to the lower end of the double tube section. Without hot gas circulation this lower end will fail to melt the adjoining rock and, once bored into the soil, will remain held in position. The problem of subsidence and material addition is thought to be avoided with sensible energy storage suggesting that it may lead to simpler deployment.

In addition to containment, insulation of the TSM will also be a consideration. The lunar regolith itself is a reasonably good thermal insulator [10], particularly at low temperatures. It consists of small granules of rock lying in an extremely high vacuum. Packings of such rocks result in what is termed "point" contact. While rocks may touch over a larger area than single points, the thermal contact is not intimate and provides an extremely poor path for conduction. Under these circumstances radiation becomes the predominant mechanism for heat transport. While this becomes increasingly effective at highly elevated temperatures, the soil remains a highly effective insulator. Under these circumstances there appears little reason to use anything other than available materials for insulation purposes. Insulation at the lunar surface may be enhanced through the use of radiation shields. Since these are typically low weight, compact sized elements, they should not play a significant part in establishing the delivered load.

An additional consideration in locating the system will be that the regolith be sufficiently deep to provide the insulating effect of the soil. Apollo missions have shown the depth of the regolith is quite variable. This variation is shown in Figure 6. Measured values range from a minimum of 3 m in the mare region to a maximum of 15 m [11] as measured in the basin ejecta. Below this depth, bed rock was found in the mare region but a more consolidated, less porous regolith was encountered in the basin ejecta. The design proposed here will require a regolith depth of 7 to 8 m for latent energy storage or 14 to 15 m for sensible energy storage to provide sufficient thermal insulation below the TSM. Where sites are judged as being unsuitable due to poor insulating capabilities, mine tailings may be utilized.

The proposed design is thought to provide several features. First, by the extensive

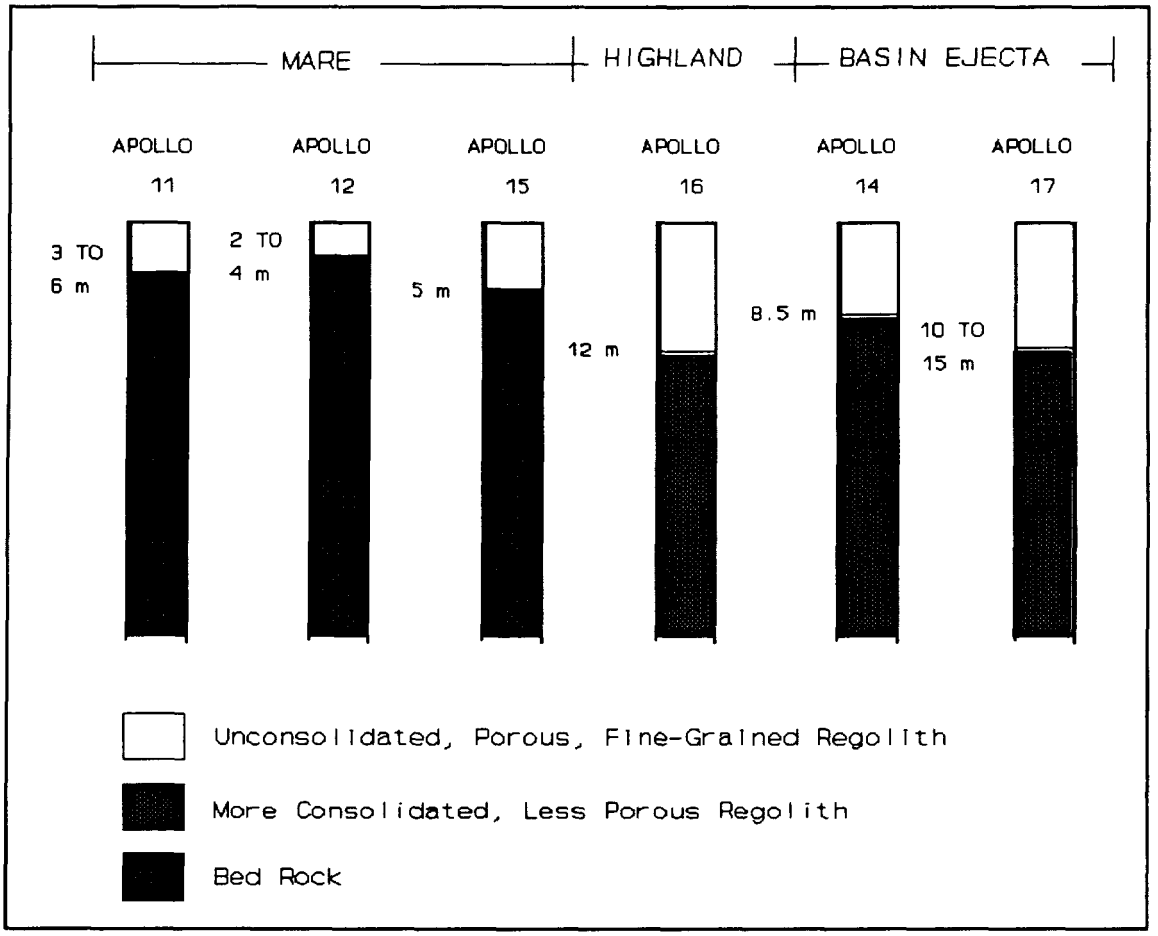

Figure 6. Depth of Lunar Regolith at the Apollo Landing Sites. [11]

use of native materials, transport costs and logistical problems are minimized. The system is designed to be compact during the launch period and can be deployed without specialized connecting equipment or skills.

3. Analysis

The intentions of the analysis performed in the course of the study were to (a) verify the cyclic operation of the proposed system, (b) determine the start up requirements, (c) ascertain overall system launch weight and (d) evaluate the feasibility of the proposed TES heat exchanger system. The focus will continue to be on critical aspects of performance.

3.1 TES Heat Exchanger

During the previous study of the co-generation concept, considerable attention was given to the design of the TES heat exchanger concept. The problems of deployment were never completely resolved so that consideration has extended to this study in an attempt to obtain a design which could directly answer all concerns. Much of the difficulty with this earlier design, dealt directly with its larger size; the co-generation unit provided an equivalent of 62 kW of continuous power as compared with 25 kW_e for the electrical generation concept. This larger design will, naturally, require a significantly larger TSM volume. The resulting design called for a TSM depth of about 15 m, too long to allow direct, full length transport from Earth. One design approach was to transport the heat exchanger as shorter segments, to be assembled on site. The problem then was finding suitable materials and associated leak proof joining methods.

The electrical power generation system now under consideration may present a somewhat simpler problem. The required heat exchanger length is markedly smaller for latent energy storage, being only 4.19 m. For the sensible energy storage system this length up to 10.44 m, probably will require a compacted tube for transport. Either a latent storage system or some combination latent and sensible storage concept may permit transport as a single section. This arrangement might permit use of either refractory metals, being relatively easy to join, or ceramic materials, offering higher temperature strength and corrosion resistance. The sensible energy storage system, due to its excessive length, is thought to require the elastic deformation or joinability of a metal. Refractory metals were preferred for the co-generation concept and a similar design is selected here. The configuration used previously incorporated a hexagonal array of straight vertical tubes. Thirty seven to sixty one such tubes, depending on the tube pitch selected, placed 0.643 or 0.5 m on center, respectively, would serve to provide

adequate coverage of the areas proposed. The larger number of tubes would provide a more uniform temperature throughout the TES and at the turbine inlet; conversely, the larger number of tubes significantly complicates the fabrication/deployment problems so that a trade-off between these two considerations would be required.

Table IV. Primary Gas Energy Transport System Design Conditions.

Energy transport rate.	203 kW
Design gas temperature change.	200 K
Gas composition	He-Xe mix
Equivalent molecular weight	38
Specific heat	2.19 kJ/kg K
Mass flow rate	0.46 kg/s
Avg. max. gas temperature	1600 K
Pressure	2.21 atm
Gas density	6.40 kg/m^3

An alternate configuration would be to incorporate a smaller number of helical spiral tubes. By spiraling several concentric tubes about the central axis of the TSM volume, efficient energy distribution can be achieved as effectively as with 6 or 12 straight tubes. This is the method being proposed here. The TSM volume has been subdivided into 4 radial zones as shown in Figure 7. These are sized so that the radial length of thermal penetration into the TSM from each tube will be equal. The central cylinder is taken as having a 1.125 m diameter and will have the spiral heating tube located at a mid radius of 0.28125 m; this allows for energy to travel equal distances in the inward and outward radial direction. Similarly, each of the three surrounding annuli will have a thickness of 0.5625 m and will have the heater located at mid radius for the annulus. A single helical coil tube is to serve as the heat exchanger for each zone. In this fashion, the four tubes replace the 61 required for an equivalent tube to tube pitch with a straight tube design. Overall coolant requirements are assumed as shown in Table IV. The distribution of coolant to each of the helical tubes is in proportion to the associated volume of TSM. Using the assumed gas flow conditions shown in Table III, each of the heat exchanger tubes is sized to achieve equal temperature rises and equal gas velocities.

3.1.1 TES Heat Exchanger Stress Analysis

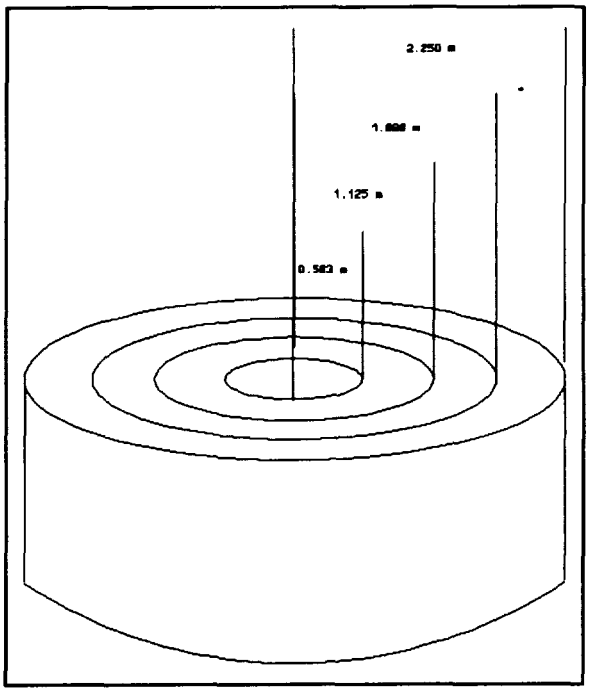

Figure 7. Heating Zones for Thermal Storage Material.

The objective of the design is to permit these helical coils to be fully compressed to a minimum volume for launch and then deployed on the lunar surface. The limits for the design will be that the coils should not be stressed to exceed the elastic limit at standard temperature conditions under compression for launch nor under extension for deployment. In this case it is assumed that the no load conditions will lie mid way between these two extremes. For the limiting condition, when compressed for launch, each tube should be at its elastic limit; when extended for deployment each tube will be stretched to its elastic limit. In addition, it will be required that the tubes not exceed the internal hoop stress caused by the pressurized working gas under high temperature conditions. From basic stress considerations, it is found that the parameters affecting the maximum stress include the helix diameter, the helix pitch, the pipe wall thickness and the pipe diameter. Basically a small helix diameter leads to large deflection stresses; a large helix pitch, pipe wall thickness or pipe diameter likewise lead to large deflection stresses.

The results of the stress analysis are shown in Table V for tubes in the innermost and in the outermost zones. Since the heat exchangers define a set of annular flow passages, two concentric tubes are actually used in each heat exchanger coil. In each case the outside tube will be subjected to the larger stresses so that only the single tube need be analyzed.

Table V. Full Deflection Stresses for TES Heat Exchanger Tubes.

	Zone 1	Zone 4
Mass Flow Rate, kg/s	0.03	0.21
Tube ID, m	0.0219	0.0547
Tube OD, m	0.0255	0.0582
Mod. of Elasticity, kN/m^2	$1.79x10^8$	$1.79x10^6$
Poisson's Ratio	0.3	0.3
Maximum Deflection, m	1.83	1.81
Coil Diameter, m	1.125	3.9
Coil Pitch, m	0.175	0.400
Hoop Stress, kN/m^2	$1.59x10^4$	$1.35x10^4$
Deflection Stress, kN/m^2	$1.38x10^5$	$1.52x10^4$
Compressed Length (Latent Storage), m	0.61	0.61
Compressed Length (Sensible Storage), m	1.52	1.52

The gas pressure has been adjusted so as to maintain the hoop stress in Zone 4 below $1.35x10^4$ kN/m^2. This basically corresponds to the high temperature stress limit for tantalum. While other material may actually be preferable, this analysis does indicate that by either adjusting gas pressure or alternately thickening the wall on the outer most zone, the system can accommodate anticipated stress levels without requiring excessively thick walls or low pressures. Similarly the deflection stress in Zone 1 is maintained below $1.38x10^5$ kN/m^2, corresponding to the low temperature elastic limit. It was found during the analysis that the deflection stress could always be reduced by reducing the coil pitch. This adjustment, while increasing the compressed length of the coil for launch and consequently the coil weight, serves the additional function of improving the heat distribution within the TSM. Note that this configuration provides for a relatively small launch envelope 3.9 m in diameter and 0.61 m tall.

3.1.2 Solar Dynamic System Weight

The proposed system will use many of the same components as previous Solar Dynamic Systems. In particular the concentrator, Brayton engine & generator, radiator and frame will largely duplicate those shown in earlier studies [1]. The total mass for these components based on a 25 kW_e system is 1278 kg. Additional components required here will include the Brayton Cycle heat exchanger, heat receiver, TES piping and circulation loop.

The TES coil heat exchanger size is calculated as shown in Table V. The overall system mass flow is sized to provide a 250 K temperature change across the TES heat exchanger. Flow is distributed to each zone of the TES so that the flow is directly proportional to the storage volume. The coiled heat exchanger tubes are designed to provide a gas velocity of 30.48 m/s (100 ft/s) with tube wall thicknesses of 1.778 mm. The coil in Zone 1 is stress limited by the distortion in compression and extension. This requires a relatively large number of coils to avoid exceeding of the elastic limit. All other tubes are sized to provide a tube to tube pitch of 0.06 m as determined from thermal considerations. Based on these conditions the overall mass of the TES heat exchangers is found to be 1066 kg for latent storage. Accounting for the additional length required for sensible storage, the overall heat exchanger weight would be 2737 kg. In either case this represents the single largest mass in the system. The outer coils are clearly heavier due to both the larger tube diameter and greater helix diameter. A higher molecular weight gas mixture might be considered to reduce the required tube flow area and to permit higher operating pressures. This approach would require either different mixtures for the TES and Brayton cycle working fluids or a modification of the reference working cycle. Further consideration of this approach is postponed for future evaluations.

TABLE VI. TES Heat Exchanger Design Characteristics.

	Zone 1	Zone 2	Zone 3	Zone 4
Mass Flow,kg/s	0.028	0.085	1.14	0.208
Velocity, m/s	30.48	30.48	30.48	30.48
Molecular Wt.	38	38	38	38
Pressure, atm.	22	22	22	22
Temperature, K	1600	1600	1600	1600
Density, kg/m_3	6.40	6.40	6.40	6.40
Wall Thickness, cm	1.778	1.778	1.778	1.778
Inner tube ID, cm	1.362	2.359	3.046	3.683
Inner tube OD, cm	1.718	2.715	3.116	4.039
Outer tube ID, cm	2.192	3.597	4.566	5.466
Outer tube OD, cm	2.548	3.653	4.922	5.821
Metal Density, kg/m^3	8570	8570	8570	8570
Mean Helix Diameter, m	1.125	2.050	2.975	3.9
Length, m	42.36	86.69	86.69	86.69
Mass	79.30	262.0	330.7	394.4

System mass estimates are shown in Table VII and, with the exception of the concentrator, frame radiation shields and TES heat exchanger, taken directly from previous studies [12]. The methods for sizing the concentrator and frame are taken from the same source, but masses are re-established for the proposed concentrator size. Radiation shields are assumed to be constructed from niobium, 7 m in diameter, and with a thickness of 0.019 mm per layer. The mass of any associated spacers is assumed negligible (R. Jetley, Aerospace Design and Development Co., Personal Communication).

The overall system mass is calculated to total just over 3600 kg, or 144 kg/kW, for latent storage; 5279 kg or 211 kg/kW for sensible storage. This is somewhat over that of previous studies, being attributed to the closer spacing of heat exchangers and more uniform distribution of energy, but it is still less than one half the published values for existing alternatives.

TABLE VII. Component Weights for Solar Dynamic Power Generation System.

Concentrator	250	kg
TES HX (latent storage)	1066	kg
TES HX (sensible storage)	2737	kg
Brayton Cycle HX	93	kg
Radiation Shields	825	kg
Compressor	10	kg
Engine & Generator	664	kg
Radiator	256	kg
Frame Mass	445	kg
Total Mass (latent storage)	3608	kg
Total Mass (sensible storage)	5279	kg
Specific Weight (latent storage)	144	kg/kW
Specific Weight (sensible storage)	211	kg/kW

3.2 Thermal Analysis

Start-up of the in-situ TSM will be the most critical aspect of the design. Unlike prefabricated systems, the designer has no real control over the thermal characteristics of the insulating material, in this case the surrounding soil. While the lunar soil provides excellent insulation during the established cyclic operation, it does comprise a substantial

mass and exhibits a relatively large specific heat. During the start-up transient it is not only the TSM which must be brought to the operating temperature, but also this surrounding mass. This represents a substantial energy sink which must be initially satisfied before sustained cyclic operation can be attained. Care must be taken to ensure that the system is designed to provide for this parasitic start up load.

An analyses has been performed of the start up of this system and the results are presented in this section. This study utilizes a one dimensional radial, transient analysis. Properties of lunar materials used throughout these calculations are based on the best information available at this time. The process of property selection is described in Appendix A.

3.2.1 Thermal Analysis Methods.

All analysis have been performed using the dimensional, transient, radial finite difference code described in Reference [13]. This code is designed to account for both latent and sensible energy storage but limits consideration of heat transfer by conduction only. Radiation may be included by lumping the effect with conduction by adding an equivalent temperature dependent term to the normal thermal conductivity. Convection within the liquid phase has not been considered but, in fact, may be significant for a portion of the heating process.

3.2.1.1 Thermal Model

The approach taken has been to consider two portions of the TSM as shown in Figure 8. There will be an inner core, geometrically defined as that material located radially inside of the outer most heat exchanger coil but also including that portion of soil located below the TSM which must be preheated. This will include 75% of the TSM but only about 13% of the start up parasitic load. The second region will include all TSM located outside of these same tubes and, additionally, all material located radially outside of the active TSM region.

As indicated previously, the parasitic load will lie primarily in this second region. The explanation for this is as follows: Referring to Figure 9 the parasitic volume to TES surface ratios are compared for the side and bottom of the TSM. Preliminary calculations indicate that the effective thickness of the start up parasitic region will be about 0.67 m. At this distance the temperature will drop to a value approximately mid

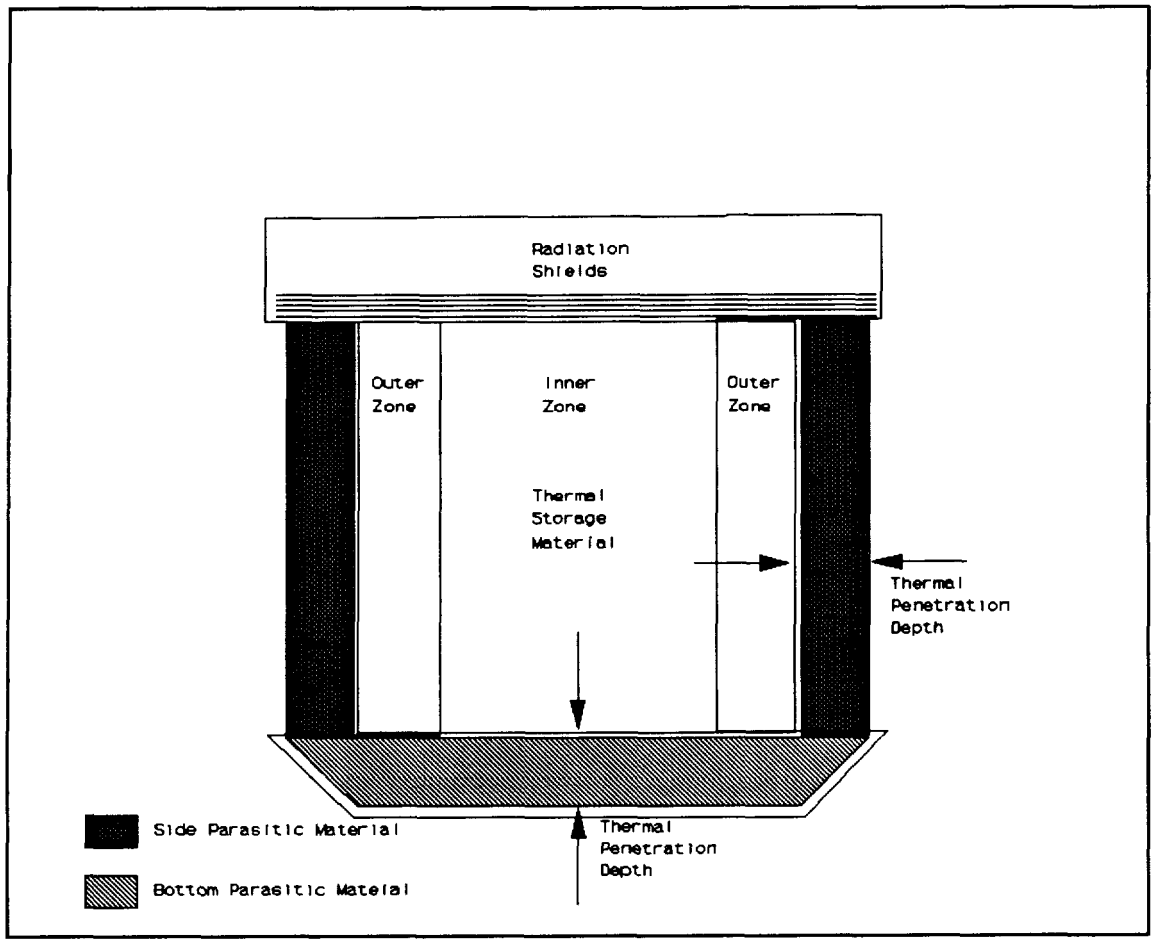

Figure 8. Distribution of TSM Used in Thermal Analysis.

way between the melting temperature and the temperature of the surrounding soil at start up. This results in a volume to surface area 1.13 times larger for the inner zone than for the outer. In the case of latent storage, the side area is approximately 7.5 times that of the bottom, leading to a parasitic heat load which is 6.65 times larger on the outer zone than on the inner. The proportion of parasitic load in the outer zone will be significantly larger with sensible heating due to the substantially longer length. With the parasitic load primarily located radially outside of the TSM and with the small thermal capacitance of the TES in this zone it is this second region which will be of primary concern during the start up transient.

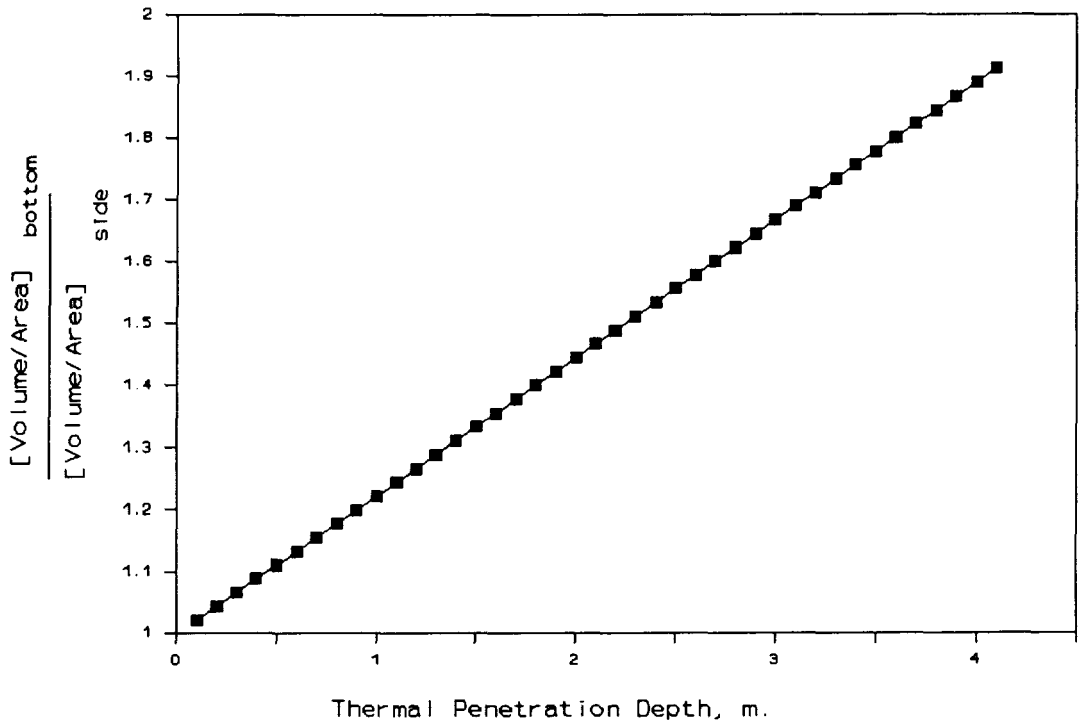

Figure 9. Parasitic Volume Ratios for Proposed TSM Arrangement.

3.2.1.2 Conduction Analysis

The finite different analysis is performed using a transient, one dimensional code designed to accommodate isothermal phase change and using an implicit convergence technique. The TES materials under consideration, being mixtures rather than single chemical species, actually melt over a temperature range of between 1325 and 1425 K. This is modeled as a single melting temperature at the mid-temperature, 1375 K, with sensible heating occurring at higher and lower temperatures.

The semi-infinite media surrounding the TES is modeled by assuming a sufficiently large radius for analysis so that with insulated boundary conditions, no measurable temperature increase occurs at the boundary. In this case the inner radius is taken as 1.95 m and the outer as 7.95 m. Thirty equi-spaced finite sections are included between these limits.

3.2.1.3 Convection Effects

Viscous effects in the low gravity environment will delay the onset of free convection within the liquid phase, but as the thickness of the melted zone exceeds the critical value some enhancement may be expected. In this case the Nusselt number has been calculated using a correlation developed [14] for free convection across rectangular cavities with the vertical walls heated:

Properties used in this calculation are shown in Table VIII.

Table VIII. Convection Properties for TES

Avg. Temp.	1375	K
Specific Heat	0.85	kJ/kg K
Density	3000	kg/m^3
Viscosity	4.60	kg/s m
Thermal Conductivity	0.0012	kW/m K
Gravitational Constant	1.62	m/s^2
Volumetric Expansion Coefficient	0.000064	1/K
Kinematic viscosity	0.001533	m^2/s
Heat Input	47.63	kW
Height	4.19	m
Heat Flux	0.93	kW/m^2

Here the calculations are performed based on a constant heat flux of the average magnitude for the outer zone used in the remainder to the thermal calculations. The predicted Nusselt number and overall temperature difference across the molten material is shown as a function of the liquid thickness in Figure 10. For thicknesses of greater than 0.1 m, the Nusselt number becomes greater than one so that some convective enhancement is achieved. Below this thickness, heat transfer is by conduction and the temperature drop increases linearly with thickness to a maximum of about 58 K. As the molten layer becomes thicker, convective effects become larger causing the overall temperature difference to decrease slightly. This suggests that the maximum heat exchanger tube wall temperatures may be limited, perhaps to about 1485 K. While this tendency toward thermal uniformity within the molten TES should enhance the stability of Brayton cycle operation and limit radiation losses through the thermal shields, parasitic losses may be increased. While this is clearly a concern in establishing the

validity of the design and will require additional evaluation.

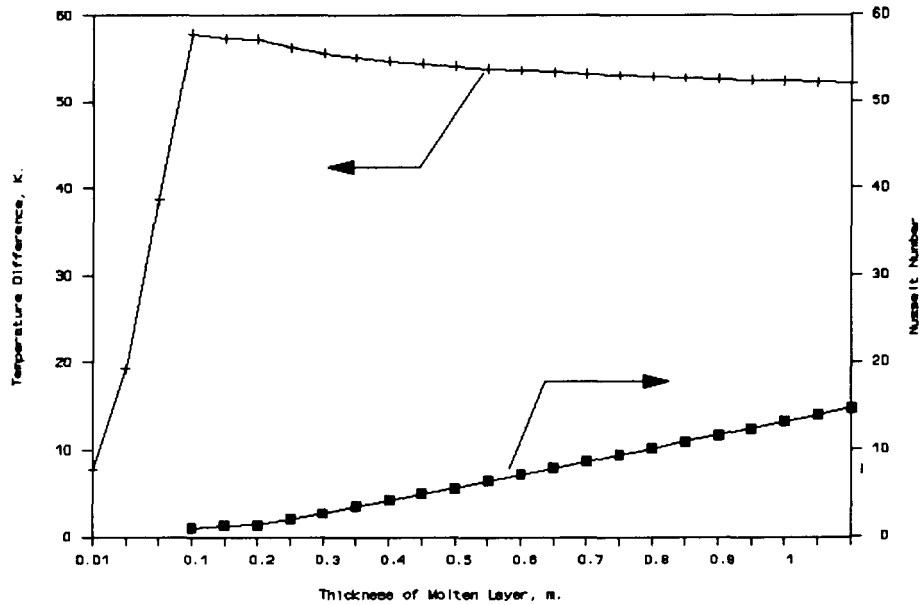

Figure 10. Temperature Drop Across Molten TES Layers.

3.2.2 Periodic Thermal Performance

Once the TES and surrounding soils are brought to operating temperature, steady periodic operation begins. The key feature of this operating condition is that no energy is required for the parasitic load; all energy input is utilized for power production or is lost to the surroundings without increasing the average temperature of the surroundings. Parameters used to size the TSM for steady periodic operation are shown in Table IX. The periodic heat losses, shown in Table X, must be determined using an iterative analysis with TSM sizing to account for that portion of energy storage to accommodate thermal losses during eclipse. Losses from the top of the TSM volume are assumed to be radiative and are limited by the use of multiple thermal radiation shields. Losses through the shields are calculated using a correlation proposed by a commercial supplier [15]. This results in somewhat larger losses than would be found from a theoretical analysis. This is due to the additional consideration of parallel loss paths through spacers located between individual heat shields. The selection of 90 heat shields is somewhat arbitrary. In this case the number selected was chosen so that radiative losses

would be a similar order of magnitude as conductive losses. Conduction losses are calculated using the methods outlined in Reference [16]. Since the method only accounts from losses from the sides of the TSM containment, the length has been increased to provide a total area equivalent to that of the physical TES system. A geometric mean thermal conductivity is used for the soil. Total losses are found to be only 7.65 kW for latent storage and 6.76 for sensible storage, both quite manageable within the overall power requirements of the system. As will be seen these losses are well below the parasitic losses during start up indicating that these transient start up losses will predominate and they will determine the overall power input requirements within the design.

The dimensions of the TES and the heat exchanger are selected to ensure that the later unit is practical, both in terms of heat transfer performance and transportability. Because of the compressibility of the coiled heat exchangers in the axial direction, it is the radius of the larger coils which are considered limiting. In this case the dimensions were selected to be compatible with cargo dimensions (John Bozek, NASA Lewis Research Center, July 22, 1990) listed for the previously defined lunar lander craft.

TABLE IX. Parameters for Calculating Steady Periodic Operation.

Latent Storage

TSM Density	3000 kg/m^3
TSM Specific Heat	1.44 kW/kg K
TSM Heat of Fusion	419 kW/kg
Electrical Power Output	25 kW
Overall Cycle Efficiency	0.31
Steady Periodic Heat Loss	7.65 kW
Cycle Period	29.5 days
Energy Storage Requirements	1.13×10^8 kJ
TSM Mass	199914 kg
TSM Volume	66.64 m^3
TSM Radius	2.25 m
TSM Length	4.19 m
Environmental Temperature	253 K
TSM Melting Temperature	1325 K

Sensible Storage

TSM Density	1800 kg/m^3
TSM Specific Heat	1.44 kW/kg K
Electrical Power Output	25 kW
Overall Cycle Efficiency	0.30
Steady Periodic Heat Loss	6.76 kW
Cycle Period	29.5 days
Energy Storage Requirements	1.15×10^8 kJ
TSM Mass	308150 kg
TSM Volume	171 m^3
TSM Radius	2.25 m
TSM Length	10.76 m
Environmental Temperature	253 K
TSM Operating Temperature	1250 K

TABLE X. Steady Periodic Losses From In-Situ TES System.

Latent Storage	
Number of Radiation Shields	90
TSM Average Temperature	1375 K
Soil Temperature	253 K
Radiation Losses	3.77 kW
Equivalent Length	5.31 m
Shape Factor	21.5
Thermal Conductivity, 253 K	0.02 W/m K
Thermal Conductivity, 1425 K	1.29 W/m K
Average Thermal Conductivity	0.16 W/m K
Conductivity Losses	3.88 kW
Sensible Storage	
Number of Radiation Shields	90
TSM Average Temperature	1250 K
Soil Temperature	253 K
Radiation Losses	2.57 kW
Equivalent Length	11.9 m
Shape Factor	31.7
Thermal Conductivity, 253 K	0.02 W/m K
Thermal Conductivity, 1250 K	0.88 W/m K
Average Thermal Conductivity	0.13 W/m K
Conductivity Losses	4.19 kW

3.2.3 Initial Start Up

Based on the steady periodic conditions, there is adequate energy to heat the TSM to it's melting temperature within two lunar months while continuing to provide full electrical power during the periods of solar incidence. However, there remains the problem of heating the surrounding soil to it's steady state value. This energy must come from the solar concentrator and will clearly delay the onset of power generation from the TES.

Preliminary calculations had shown that the system could not bring the surrounding soil to temperature from energy allocated for energy losses from the steady

periodic condition unless initial power generation was delayed. Several alternate strategies might be employed to compensate: (a) Several units might be clustered so that they can thermally shield one another; (b) Power generation might be curtailed during periods of solar incidence during initial periods of operation to bring the system to temperature more quickly; (c) Power levels during the solar eclipse might be limited so as to match initial TES capabilities; (d) The solar concentrator could be oversized to accommodate the start-up period. For a single unit, power reduction during this period would need to be about 10%, to about 22.5 kW. Alternately, an availability of about 90% could be accommodated with the available stored energy; this approach might prove an attractive strategy when the power unit is used in conjunction with a process plant where plant availability is also a limiting factor.

TABLE XI. Concentrator Requirements for 25 KW In-Situ Solar Dynamic System.

Concentrator Efficiency	0.92
Receiver Efficiency	0.85
Power Requirements	192 kW
Solar Constant	1.32 kW/m^2
Overpower	15 %
Concentrator Area	236 m^2
Concentrator Diameter	17.3 m

The approach taken in this analysis has used a combination of these strategies, curtailing initial power during the first period of solar incidence and oversizing the concentrator to accommodate the additional heat up losses. This approach ensures that full rated power is available from an early period after deployment. The concentrator has been sized to provide 15% excess area over that indicated by the steady periodic analysis, as shown in Table XI Note that the oversizing of the concentrator provides a margin of safety on steady periodic operation. If the start-up period is assumed to begin at the beginning of a lunar day, then full power operation can be commenced for periods of direct incidence at the start of the second lunar day for latent storage; power can be generated continuously starting with the eclipse in the fourth lunar day. For sensible storage power generation during periods of solar incidence is delayed until 11 earth days into the third lunar period. Power during eclipse is delayed until the fourth lunar period.

In analyzing the thermal transient during start-up, input energy is allocated as shown in Table XII. Since the analysis is to be one dimensional, consideration must be

given to the actual distribution of power from the top and sides. The assumption made here is that these losses will be allocated in the following manner. First a heat up period is assumed. Energy is allocated to the central zone to bring the TSM to temperature and to account for radiant losses during the start up period. Energy is similarly allocated to the outer zone to bring this TSM to temperature. The remaining energy is assumed to be available for parasitic losses. This energy is allocated as indicated in Figure 9.

TABLE XII. Power Distribution In One Dimensional Transient Analysis.

	Latent Storage	Sensible Storage
Start Up Period During Incidence	2 per.*	3.4 per.
Start Up Period During Eclipse	4 per.	4 per.
Total Power to TSM	122 kW	123 kW
Power Available for Losses	34 kW	41 kW
Mass Fraction in Central Zone	75 %	75 %
Power to Storage in Central Zone	68 kW	68 kW
Power to Losses in Central Zone	8 kW	4 kW
Total Power to Central Zone	76 kW	72 kW
Mass Fraction in Outer Zone	25 %	25 %
Power to Outside Zone	46 kW	51 kW
Cycle Power Input from Outer Zone	20 kW	21 kW

* A lunar period (per.) is taken as 28.5 earth days.

With this distribution the analysis proceeds as a one dimensional radial analysis of the outer zone. If the assumed start up transient is too short, parasitic losses will not be satisfied and the required start up temperature is not reached. A longer transient is then assumed and the process is repeated until system energy storage is adequate for full power production.

The start up transient temperature history for the first nine lunar periods is shown in Figure 11. The depth of penetration is seen to continue to increase through this period, but tends toward an asymptotic value near the end of the transient. The peak metal temperature is seen to be about 1650 K. This peak is reached at the end of the

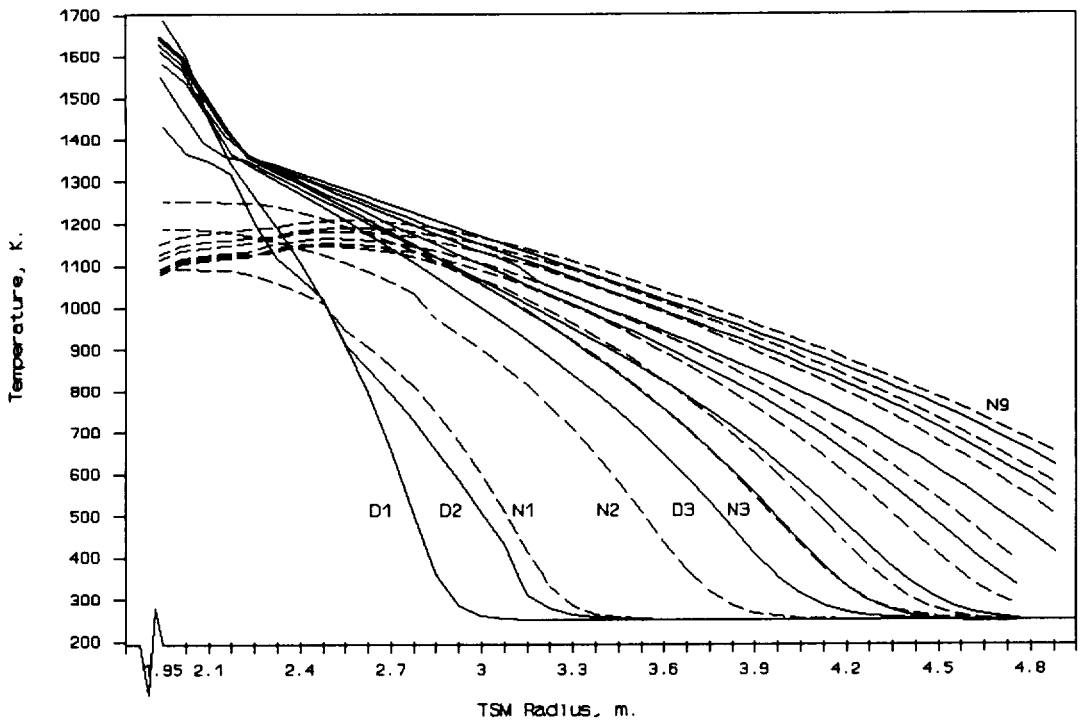

Figure 11. Start Up Temperature Transient for Latent Storage System.

first period of solar incidence, indicated by the symbol D1. A sudden change in the temperature slope is indicated at a temperature of 1375 K, corresponding to the point at which phase change is deemed to occur. During the first eclipse period, N1, the peak temperature is seen to drop to about 1100 K as the energy is transferred to a greater radius. The Brayton cycle engine is started at the start of the second incidence period so that by the end, D2, a lower peak temperature is observed. The first eclipse period with sufficient energy storage for engine operation is the fourth lunar month, N4; at this point the interior temperature is seen to drop to around 1100 K as energy is removed from the TES. As time progresses, the average and peak temperatures in the outer zone are seen to continue to increase during both eclipse and solar incidence; this is an indication of the overpower associated with the increased size of the solar concentrator.

After continuous engine operation is initiated, the analysis indicates that the TSM temperature drops to a level of between 1100 and 1150 K. This temperature is somewhat low for engine operation but it should be noted that the energy allocation provides for the central zone with the bulk of the TSM mass to drop to only 1325 K; the average engine operating temperature should remain near the design level.

The start up transient for the sensible storage system is shown in Figure 12. The

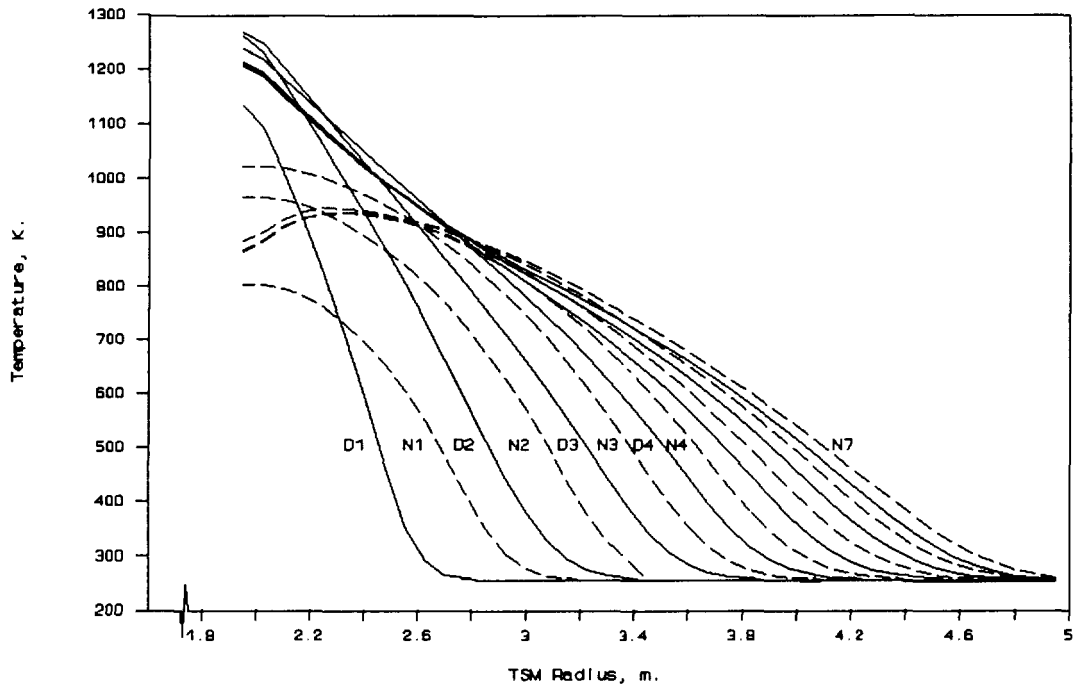

Figure 12. Start Up Temperature Transient for Sensible Storage System.

peak temperatures are about 1250 K and are approached during the second lunar day. This is a significant reduction from the peaks observed for latent storage suggesting that this approach may result in much less severe heat exchanger temperatures. The reduction is only partially due to the lower operating temperature; the longer TES section also reduces the system heat flux providing for lower temperature gradients. Power generation begins during the period of solar incidence during the fourth lunar month. After this time the peak temperatures during eclipse is seen to drop to between 900 and 950 K. Again this is partially an artifact of the analysis method so that central zone temperatures will tend to maintain the overall system nearer 1000 K. As time progresses the transient isotherms begin to lie closer together on the graph indicating that an asymptotic value is being approached. The system should stabilize at temperatures slightly above those indicated as steady periodic operation is reached.

3.3 MATERIALS

Throughout this study the question as to what materials might be selected for use at such elevated temperatures has remained. It is thought that several ceramics could be proposed which would withstand the elevated temperatures, but they are judged

unsuitable within the context of the current design because of the need to compress the heat exchanger coils. Refractory metals come quickly to mind, in particular Niobium and tantalum seem to have adequate strength characteristics at the elevated temperatures. While structural properties appear similar, niobium is generally preferred because of its lower costs. The potential problem with either material is their tendency to oxidize rapidly at elevated temperature.

Recognizing the problem of high temperature oxidization in aircraft engines, the decision was made to contact experts in those industries for suggestions and guidance. It was suggested that augmenters are designed to operate at temperatures approximating the 1425 K design limit under conditions of near Mach 1 velocities and oxygen concentrations well in excess of stoichiometric. The surfaces used are niobium metals with a silicide coating. The life expectancy of such surfaces is on the order of 2000 hours. In discussing this subject, it was clear that the proposed application was sufficiently different that whatever was stated became somewhat speculative and would in any case require experimental verification. One position held that the absence of the highly erosive velocities and the lower oxygen concentrations may tend to extend the operational life under the proposed application. Another position was that in the reduced oxygen atmosphere any silicide coating would quickly disappear as silicon and oxygen reacted to form SiO, a gas. It was further stated that because of the low oxygen concentration, that no coating may be necessary. It is also noted that certain new materials are under development which may be applicable. In particular, DOD is currently funding a research effort at the University of Florida to develop and test a niobium-aluminum alloy. In this case the niobium serves to provide high temperature structural properties while the aluminum may oxidize to provide an extremely durable passivating layer on the surface. Our conclusion is that there are sufficient numbers of candidate materials to suggest that a suitable material can be found to operate within the temperature range of sensible and/or latent thermal energy storage.

Oxygen fugacity for lunar soils is known to be low as seen in Figure 13. Clearly the rate of reaction will tend to increase with temperature as would be expected. What should be noted however is that the fugacity levels for lunar basalts at 1200 to 1300 K are of the same order of magnitude as for terrestrial basalts near room temperature. This suggests that within the lunar environment systems may operate at somewhat higher temperatures, without excessive corrosion, than would be acceptable under terrestrial conditions.

4. DISCUSSION

4.1 Technical Feasibility

The first question to be addressed in considering the feasibility of an in-situ storage system is whether such a design is feasible within the energy constraints. Results shown here indicate that periodic thermal losses can be limited to relatively small values, approximately 4% of the overall power input. During the start-up transient additional parasitic losses, unique in the in-situ concept, occur and these will require careful design consideration so as to limit any adverse impact on overall design performance.

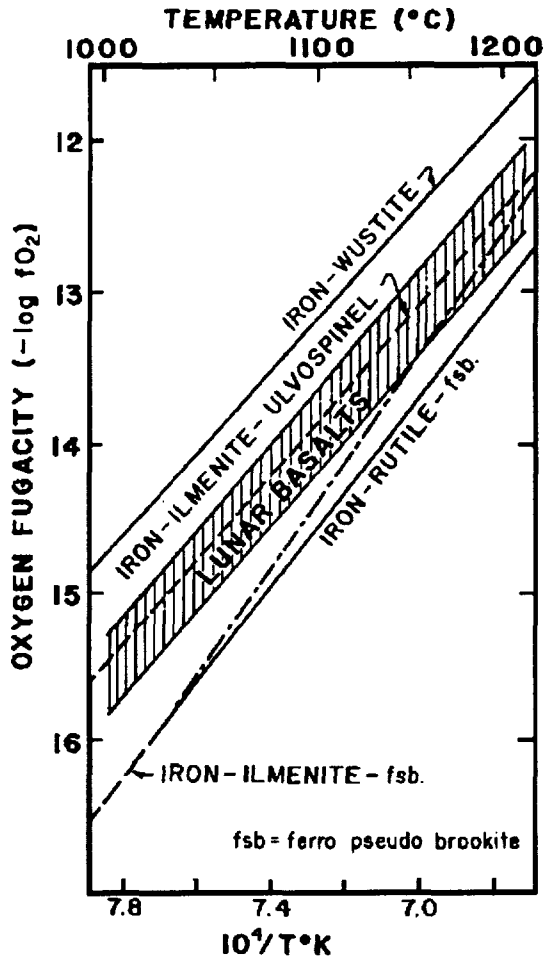

Figure 13. Oxygen Fugacity for Lunar Basalts. [5]

While sufficient power is available from the concentrator to bring the TES up to operational temperature within 2 lunar months, the presence of the parasitic losses delays operation from thermal storage for an additional 2 lunar months. While this delay is clearly to the detriment of in-situ storage it is not necessarily unacceptable nor is the heat up problem clearly a critical path item. Moreover, this start up period may be shortened or lengthened, depending on the extent of overpower to be built within the solar concentrator, the start-up sequence and the relative positions of additional units. With the designs proposed concentrator power levels are increased 15% over those required for established periodic operation. This results in an overall input power level of 192 kW_t for 14.75 days to produce a net output of 25 kW_e for 29.5 days, resulting in an overall system efficiency of 26%. This is considered to be comparable to alternative power technologies and should not suggest an overly large or heavy concept.

The overall specific weight is found to be 144 kg/kW for latent storage, 211 kg/kW for sensible. Either design compares favorably with the published values for PV with cryogenic storage, approximately 300 kg/kW or PV with pressurized storage at approximately 600 kg/kW. It is the potential for large delivery weight and volume savings that provide an incentive for development of the concept. This study indicates that this potential continues to be quite large and the design could offer substantial advantages in the development of any future lunar base.

The design of a deployable system has been addressed only in terms of the heat exchanger. The largest sized component of the system will clearly be the concentrator; this component has been extensively studies elsewhere and is not included in this evaluation. After the concentrator, the TSM heat exchanger will be the next large sized component. A concept for a collapsible helical coiled heat exchanger have been presented and stress analysis has show that such a component could be constructed within the design requirements of the system. The implication is that a prefabricated, collapsible, large volume heat exchanger could be designed and constructed to fit within a small portion of the proposed lunar landing vehicle. Moreover such a heat exchanger could be fabricated from materials which are most compatible with the lunar soil.

Materials for the heat exchanger present what is judged to be the critical technological issue for the design concept. The temperatures required for latent storage are judged high by normal engineering standards. In particular the high temperatures will restrict heat exchanger material suitability. Most likely high temperature ceramic materials will react chemically with the molten magma in the latent storage concept. This limits consideration to high temperature steels and refractory materials. Candidate materials include Niobium, tantalum, molybdenum, and their alloys. No final determination can be made without direct testing under simulated lunar conditions. In any case the difficulty of material selection will be directly related to the peak temperatures and cyclic variations. These can be alleviated to some extent by adding additional concentric heating coils, reducing the required local heat flux. However, under any circumstances, the successful, long term operation of any refractory metal under the extreme conditions would require careful demonstration. Sensible storage is seen to reduce these peak temperatures to a range which is within that normally proposed for solar dynamic systems.

High temperatures will also lead to quite stringent standards on concentrator accuracy or will result in relatively large focusing and aperture losses. These problems are not considered to be critical in regard to the feasibility of the concept, but may

directly impact the design goals of concentrator size and weight. This project can directly benefit from ongoing concentrator efforts; conversely, to the extent that this project might lead to improved concentrator performance, spin offs of this program may directly benefit terrestrial and space related solar technology.

4.2 Trade-Offs Between Latent and Sensible Storage

Throughout this study the two storage concepts have been kept largely distinct. Two advantages occur as a result: (1) Unique advantages of each approach is accentuated and (2) the analysis can proceed with clearly established parameters avoiding the complexity of relative trade-offs. The first of these is thought to provide a technically sound basis for the approach taken. The second simply delineates the boundary from where this study has ended and any subsequent study might begin.

4.2.1 Advantages of the Alternate Design Approaches

Latent storage is clearly the lighter and more compact of the two designs. Because of the larger heat exchanger associated with sensible storage, the design would be about 30% heavier for the same power output. Moreover the heat exchanger tubes, clearly one of the larger components to be transported, are only 40% the size of the sensible storage concept. These features provide a clear and compelling reason to prefer latent storage in any development effort. However, the higher temperatures encountered with latent storage clearly represents a distinct technological development risk. Sensible storage provides a convenient fall back position for the technology. The lower temperatures suggests that the materials problems should be manageable at some temperature level. Moreover the technological development programs for either approach would be quite similar and technology development can proceed together until most of the design is developed. While weight and size considerations clearly make sensible storage a second choice, it continues to offer substantial performance advantages over other candidate technologies.

Either in-situ design is somewhat restrictive as to location. The latent storage design will be relatively tolerant of regolith depth but restrictive in regard to soil chemistry. Regolith depths of greater than 7 m are shown to be adequate so that thermal penetration through the insulating regolith layer and into higher conductivity bedrock can effectively be avoided. However soil chemistry requirements may be

relatively restrictive in regard to sites unless partial melting of Olivine basalts is included. It appears from existing lunar soil samples that low MgO levels can be found in the vicinity of probable mining operations but chemical compatibility of the soil with the high temperature heat exchanger tubes may further restrict site requirements. Clearly an evaluation of this problem based on existing soil samples must await further information on materials development.

Sensible storage omits the special soil chemical concerns of latent storage but will require a site with moderately deep regolith. The deeper regolith may be obtainable within the basin ejecta, but such sites appear rare within the mare regions. This may require that thermal storage sites be constructed by moving regolith to the proposed location. This is not necessarily a disadvantage around mining areas where material movement is a normal part of the operation; spoil sites may provide ample material without substantial effort. The absence of major subsidence around sensible storage locations could provide substantial advantages where sufficient regolith depth occurs naturally and where soil moving equipment is not available.

4.2.2 Combined Latent/Sensible Storage

Hybrid systems combining the full latent storage range with an additional lower temperature sensible storage would serve to further reduce TES volume. Direct effects would be to reduce the required heat exchanger size, to reduce the start up transient interval and to reduce the parasitic volume.

APPENDIX A.

THERMOPHYSICAL PROPERTIES

Lunar soil samples were collected during the 6 successful manned lunar landings, Apollo 11, 12, 14, 15, 16 and 17. Each sight represented a distinct geological region, providing unique insights into the characteristics of the lunar environment. Given the surface area of the lunar surface and the limited number of missions in which soil samples have been taken, it is clear that an attempt to define thermal transport properties would include a large degree of uncertainty. Yet the final performance of any in-situ thermal energy storage system is directly related to those conditions.

The previous experience with developing power generation systems for a Ilmenite reduction plant has suggested that data from certain of these missions might be given precedence. If the lunar mission includes a requirement for oxygen production, it is likely to be built in a region where high grade Ilmenite ores are found. A partial listing of pertinent chemical concentrations in specific samples [5] is seen in Table XIII. High concentrations of TiO2 and FeO are an indicator of the presence of high grade Ilmenite (FeTiO3) ore. The Apollo 11 site indicates a relatively high concentration of the desired materials and also indicates a somewhat lower than average concentration of MgO, suggesting a relatively low melting temperature range. Apollo 17 sites are also considered suitable for such a mining operation; the single sample, 71055, taken from one of the Apollo 17 sites, is indicative of the high concentrations. An additional advantage of the Apollo 17 site is that it is found in the highlands region where the un-compacted Regolith thickness has been found to be greatest. The un-compacted soils should not only simplify the actual mining operation, but will also provide a high degree of insulation for thermal energy storage.

Our procedure for selection of the pertinent thermophysical properties data will be to give preference to Basalts with high Ilmenite concentrations from either the Apollo 11 or 17 sites. Where such data is not available, data may be taken from any site, with preference given to basalts with low Olivine basalt content. A second consideration will be, where ever possible, to utilize correlations proposed by Colozza (A. Colozza, Sverdrup, Personal Communication, April 8, 1991). Reviewing these correlations has shown that they are exceptionally well researched and probably represent the best information currently available. While these correlations are generated from a

necessarily limited data base, they tend to show close correlation with accepted properties of terrestrial basalts and magmas, tending to corroborate their predictions.

Table XIII. Chemical Composition of Lunar Regolith.

	Apollo 11	Apollo 12	Apollo 14	Apollo 15	Apollo 16	Luna 16	Luna 20
SiO_2	42.04	46.40	47.93	46.61	44.94	41.70	45.40
TiO_2	7.48	2.66	1.74	1.36	0.58	3.38	0.47
Al_2O_3	13.92	13.50	17.60	17.18	26.71	15.33	23.44
FeO	15.74	15.50	10.37	11.62	5.49	16.64	7.37
MgO	7.90	9.73	9.24	10.46	5.96	8.78	9.19
CaO	12.01	10.50	11.19	11.64	15.57	12.50	13.38
Na_2O	0.44	0.59	0.68	0.46	0.48	0.34	0.29
K_2O	0.14	0.32	0.55	0.20	0.13	0.10	0.07
P_2O_5	0.12	0.40	0.53	0.19	0.12		0.06
MnO	0.21	0.21	0.14	0.16	0.07	0.21	0.10

Thermal Conductivity

The thermal conductivity of a lunar soil is certainly one of the more important properties to be considered in this analysis, but also one which is subject to considerable uncertainty. It will depend on (1) the soil composition, (2) temperature and (3) soil compaction. Composition as used here will include both the chemical composition and physical composition. As igneous rocks are formed, crystallization structure will be determined by the cooling history. This, in turn, is established by the depth of the magma flow, the rate of external cooling and the position within the layer. We assume that these parameters are adequately described by the sampling site so that it is the later two parameters which will be of greatest concern.

Available thermal conductivity data for lunar samples is largely limited in temperature range to values corresponding to between 300 and 450 K. Current theory suggests that these data can be described by a general equation of the form:

The k_c term represents a temperature independent thermal conductivity component; the k_r term corresponds to a temperature dependent equivalent conductivity attributable to

thermal radiation between soil granules. The procedure used is to evaluate the two equation constants, k_c and k_r over the limited range and extrapolate to higher temperatures. In this case data must be extrapolated to temperatures as high as 1325 K, where the phase change is thought to begin. While both k_c and k_r might be expected to vary slowly with temperature, the range of extrapolation is large enough to be of direct concern. In the absence of extended experimental results use of these correlations represent the best data available. The choice here will be to utilize Colozza's correlation developed for Apollo 17 samples:

$$k(T) = 0.01281 + 4.431x10^{-10}\ T^3\ (kW/mK)$$

Once the basalt has melted and consolidated, contact resistance will be eliminated between individual granules, tending to increase conduction while the effects of radiation are expected to be reduced. Murase [17] developed data for melted and consolidated simulated lunar basalts. A curve fit of his data is represented as:

$$k(T) = 3.615 - 0.00534\ T + 7.01x10^{-6}\ T^2 - 5.8x10^{-9}\ T^3 + 1.75x10^{-12}\ T^4\ (kW/mK)$$

Specific Heat

Available data for specific heat is also limited, in this case to temperatures between 100 and 350 K [18]. Through this range c_p is seen to increase from about 0.265 to 0.83 kJ/kg K for fine grained igneous rocks. Colozza has chosen to extrapolate this data to the higher temperature range and has obtained the following correlation:

$$c_p = -1.8485 + 1.04741\ x\ \log(T)\ (kJ/kgK)$$

Integrating this equation over the temperature range of 250 to 1350 K yields an average specific heat of 1.44 kJ/kg K. This is in the range of values suggested by Yoder [19] for terrestrial basalts, 1050 to 1450 kJ/kg K, so that the projection appears valid. The effect of using the average terrestrial values would be to increase the TES required by about 5% while increasing the start-up transient by about 10%. The difference is considered marginal in a study of this type and Colozza's correlation has been selected.

Density

Samples of soil densities from the Apollo 15 and 17 missions indicate a Regolith density of between 1600 and 2000 kg/m^3 at depths below 5 to 10 cm [5]. Individual rock densities of about 2875 and 2950 kg/m^3 are reported for the highlands and maria basalts, respectively. Typically such rocks will include a large number of internal voids, sometimes associated with escaping gases. Adjusting for porosity, solid rock densities of 3300 to 3400 kg/m^3 may be expected [20]. Corresponding liquid densities of about 3000 kg/m^3 are considered typical.

Volumetric Expansion Coefficient

While the volumetric expansion coefficient will depend on the chemical composition of the soil sample, values tend to fall within a relatively narrow range of 40-60x10^6 for terrestrial basalts. Herbert [7] recommends the value:

$$\beta = 40 \times 10^{-6} \frac{1}{T} \ (1/K)$$

Magma Viscosity

Magma viscosities for lunar materials have been determined to be significantly below those for corresponding terrestrial magmas [21]. Measured values have been obtained at temperatures between 1568 and 1723 K. These are above the range of interest so that the following correlation is from an extrapolation of available data,

$$\mu = 51750 \, e^{-(T-273)/157} \ (Ns/m^2)$$

following the slopes of curves from terrestrial magmas.

References

1. R. A. Crane & M. O. Dustin, "Solar Dynamic Power/Process Heat Generation for the Proposed Lunar Oxygen Production Plant", 3rd ASME/JSME Thermal Engineering Joint Conference, March 17-22, 1991, Reno, Nev.

2. W. E. Wallin & M. O. Dustin, "Advanced Space Solar Dynamic Power Systems Beyond IOC", 22nd IECEC, Phila., PA., Aug. 87.

3. H. J. Strumpf & M. G. Coombs, 'Advanced Heat Receiver Conceptual Design Study', NASA CR-180901, Dec. 87.

4. Charles A. Lurio, "Advanced Stirling Receiver Development Program", NASA Cortractor's Report 185281, July 1990.

5. S. R. Taylor, Lunar Science: A Post-Apollo View, Pergamon Press, New York, 1975, pp. 195-7.

6. J. W. Minear & C. R. Fletcher, "Crystallization of a Lunar Magma Ocean", Proceedings of the Ninth Lunar and Planetary Science Conference, Houston, Texas, March 12-17, 1978, pp. 263-283.

7. F. Herbert, M. J. Drake & C. P. Conett, "Geophysical and Geochemical Evolution of the Lunar Magma Ocean", Proceedings of the Ninth Lunar and Planetary Science Conference, Houston, Texas, March 12-17, 1978, pp. 249-262.

8. G. Heiken, D. Vaniman & B. M. French, Lunar Sourcebook; A User's Guide to the Moon, Cambridge University Press, Cambridge, 1991, pp. 140-142.

9. J. C. Rowley & J. W. Neudecker, "In-Situ Rock Melting Applied to Lunar Base Construction and For Exploration Drilling and Coring on the Moon", Lunar Materials, Lunar and Planetary Institute, Houston, 1985, pp. 465-477.

10. Richard A. Robie et. al., "Specific Heats of Lunar Surface Materials from 90 to 350 Degrees Kelvin", Science, Vol. 167, January 30, 1970, p 749-50.

11. William C. Phinney et. al., "Lunar Resources and their Utilization", Space-Based Manufacturing from Nonterrestrial Materials, AIAA, 1977, p 97-123.
12. "Solar Concentrator Concepts for Lunar Applications", Advanced Manufacturing Center, NASA Lewis Research Center Contract #NCC3-77, April 5, 1990, p 29.

13. R. A. Crane, "Thermal Evaluation of Advanced Solar Dynamic Heat Receiver Performance", NASA LeRC CR 185117, March 1989.

14. MacGregor, R. K. & A. P. Emery, "Free Convection through Vertical Plane Layers: Moderate and High Prandtl Number Fluids", J. Heat Transfer, Vol. 95, p. 543, 1973.

15. W. R. Determan et. al, "MULTI-FOIL Thermal Insulation for the Dynamic Isotope Power System", 24th IECEC, Wash., D.C., Aug. 1989.

16. F. P. Incropera & D. P. DeWitt, **Introduction to Heat Transfer**, Wiley, New York, 1990, pp. 180-182.

17. T. Murase & A. R. McBirney, "Thermal Conductivity of Lunar and Terrestrial Igneous Rocks in their Melting Range", Science, Vol. 170, Oct. 9, 1970, pp. 165-167.

18. R. A. Robie, B. S. Hemmingway & W. H. Wilson, "Specific Heats of Lunar Surface Materials from 90 to 350 K", Proceedings of the Apollo 11 Lunar Science Conference, Vol. 3, 1970, pp. 2361-2367.

19. H. S. Yoder, Generation of Basaltic Magma, National Academy of Sciences, Washington, D. C., 1976, pp. 71-72.

20. K. I. Horai & N. Fujii, "Thermophysical Properties of Lunar Materials Returned by Apollo Missions", The Moon, Vol. 4, 1972, D. Reidel Publishing Co., Dordrecht, Holland, pp. 379-407.

21. T. Murase & A. R. McBirney, "Viscosity of Lunar Lavas", Science, Vol. 167, 1970, pp. 1491-1493.

NASA
National Aeronautics and Space Administration

Report Documentation Page

1. Report No.	2. Government Accession No.	3. Recipient's Catalog No.
NASA CR 189054		

4. Title and Subtitle
Evaluation of In-Situ Thermal Energy Storage for Lunar Based Solar Dynamic Systems

5. Report Date
March 1991

6. Performing Organization Code

7. Author(s)
Roger A. Crane

8. Performing Organization Report No.
None

10. Work Unit No.
506-41-31

9. Performing Organization Name and Address
University of South Florida
Tampa, Florida 33620-5350

11. Contract or Grant No.
NAG3-851

13. Type of Report and Period Covered
Contractor Final Report

12. Sponsoring Agency Name and Address
National Aeronautics
& Space Administration
Lewis Research Center
Cleveland, Ohio 44135-31911

14. Sponsoring Agency Code

15. Supplementary Notes
Project Manager, Miles O. Dustin
Power Technology Division
NASA Lewis Research Center

16. Abstract

A practical lunar based thermal energy storage system, based on locally available materials, could significantly reduce transportation requirements and associated costs of a continuous, solar derived power system. The concept reported here is based on a unique, in-situ approach to thermal energy storage. In this study the proposed design is examined to access the problems of start-up and the requirements for attainment of stable operation. The design remains, at this stage, partially conceptional in nature, but certain aspects of the design, bearing directly on feasibility, are examined in some detail. Specifically included is an engineering evaluation of the projected thermal performance of this system. Both steady state and start-up power requirements are evaluated and the associated thermal losses are evaluated as a basis for establishing potential system performance.

17. Key Words (Suggested by Author(s))	18. Distribution Statement
Lunar Base, Solar Dynamic Power, Thermal Energy Storage,	Unclassified Unlimited

19. Security Classif. (of this report)	20. Security Classif. (of this page)	21. No of pages	22. Price*
Unclassified	Unclassified	45	AO7

NASA FORM 1626 OCT 86

*For sale by the National Technical Information Service, Springfield, Virginia 22161